

Propagation of plasma in neon due to multiplication of background electrons

A.N. Tkachev and A.A. Fedenev

A.M. Prokhorov General Physics Institute, Moscow

Received March 27, 2008

Computational simulation of propagation of the background-electron multiplication wave (BEMW) in neon in case of 1D model is considered. In the case of spherical geometry, the BEMW speed is found. The results are compared with calculations on the base of extended diffusion-drift model.

Introduction

The ionization wave in atmospheric gas can propagate due to multiplication of background electrons of low density, always present in the gas (e.g., due to natural radiation background).¹⁻⁷ A simple mechanism¹⁻⁷ allows an explanation of the streamer propagation both to cathode and anode of the discharge gap without using the well-known photon hypothesis,⁷⁻⁹ connecting the streamer propagation with the photon transfer, followed by ionization of excited states of gas atoms.

To distinguish the gas ionization due to background electron multiplication from commonly considered ionization waves caused by the particle transfer (electron drift and conduction), it was suggested¹⁻⁷ to call the former "background-electron multiplication wave" (BEMW). In later works,¹⁰⁻¹⁵ BEMW was two-dimensionally simulated, its stability was studied, and its applicability in different fields was considered.

The BEMW propagation speed was estimated¹⁻⁷ for a number of electropositive and electronegative gases, namely, for He, Xe, N₂, and SF₆. In this work, similar¹⁻⁷ calculations of BEMW speed in neon were carried out on the base of recently obtained characteristics of electron multiplying process.¹⁶

1. Calculation of BEMW speed by analytical model

According to the theory,¹ BEMW originates near conducting nonhomogeneities of small curvature, around which the electrical field is concentrated. In this case, the wave front propagates opposite to the gradient of electric field strength modulus, and the wave front speed u_{fr} is proportionate to gas pressure and expressed via functions E_{fr}/p , universal for this gas:

$$u_{fr} = v_i r_0 / [\text{Ln} \zeta(E_{fr}/p)],$$

$$\zeta(E_{fr}/p) = \left(\frac{d \ln(u_{d,e}(E/p) \xi(E/p))}{d \ln(E/p)} \right)_{E/p = E_{fr}/p},$$

where $v_i = \alpha_i u_{d,e}$ is the ionization rate; $\text{Ln} \equiv \ln(N_{cr}/N_0)$, N_0 is the background plasma density; $u_{d,e}(E/p)$ is the electron drift speed; r_0 is the curvature of streamer head.

From data on ionization-drift parameters¹⁶ and Townsend coefficient, we have

$$\xi(E_0/p) = 43(\text{cm} \cdot \text{torr})^{-1} \times$$

$$\times \exp \left[-25.5 \left(\frac{p}{E_0} \right)^{0.5} - 7 \cdot 10^{-4} \frac{E_0}{p} \right];$$

$$u_{d,e}(E_0/p) = 7.5 \cdot 10^5 \frac{E_0}{p} \text{ cm/s}.$$

This implies the equations for BEMW front speed:

$$u_{fr} = v_i r_0 / \zeta(E_0/p),$$

$$\zeta(E_0/p) = 2 \text{Ln} \left[1 + 8.05 \left(\frac{p}{E_0} \right)^{0.5} - 7 \cdot 10^{-4} \frac{E_0}{p} \right].$$

The BEMW front speed as a function of E_0/p for Ne is shown in Fig. 1 in comparison with the earlier obtained¹⁻⁷ functions for He and Xe.

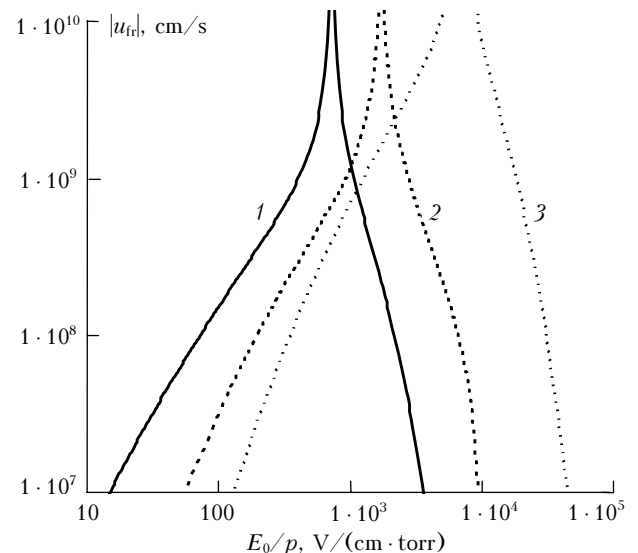


Fig. 1. The modulus of ionization front speed $|u_{fr}|$ as a function of reduced field strength E_0/p for He (1), Ne (2), and Xe (3): $N_{cr} = 10^{16} \text{ cm}^{-3}$, $N_0 = 4.5 \cdot 10^6 \text{ cm}^{-3}$, $r_0 = 0.1 \text{ cm}$, and $p = 100 \text{ torr}$.

As expected, the curve for Ne takes the position between those for He and Xe. This is concerned with

the position of ionization rate maxima for these gases, which, in its turn, depends on the maximum of ionization cross section. The reduced field strengths, at which He, Ne, and Xe ionization rates are maximal, are equal to 720, 1700 V/(cm · torr), and 7 kV/(cm · torr), respectively. As was noted in Ref. 1, the presence of singularity in the dependence of u_{fr} on E_0/p (the point, where front speed is infinite) is concerned with the presence of a maximum in the field dependence of the ionization rate. The fields $(E_0/p)_{cr}$, at which the front speed is infinite, are 720 V/(cm · torr) for He, 7 kV/(cm · torr) for Xe, and 1700 V/(cm · torr) for Ne.

2. Diffusion-drift model

To estimate reliability of analytical model's results, the ionization wave propagation in Ne was numerically calculated within the 1D diffusion-drift model, similar to that used in Ref. 17. In this model, plasma generation and screening of its external field are described by the pulse transfer equations, continuity equations for electrons and ions, and the Poisson equation.

The model describes the ionization development in the region $r_0 < r < r_{max}$ between two spherical electrodes with a common center, where r_0 and r_{max} are radii of internal and external electrodes. A homogeneous initial background and the region of enhanced initial ionization in the form of the Gaussian distribution were preset in accordance with the conditions of the analytical model.¹

The field strength dependences of variables, included in the diffusion-drift model equations (ionization rate, drift speed, and diffusion coefficients) were set on the base of approximations obtained in Ref. 16 for the electron multiplication characteristics in Ne.

For the electron $u_{d,e}$ and ion $u_{d,i}$ drift speeds, the following approximations were used:

$$u_{d,e}(E) = \begin{cases} 2.6 \cdot 10^{14} \sqrt{E/N} \text{ cm/s,} \\ \text{if } E/N \leq 4.01 \cdot 10^{-17} \text{ V} \cdot \text{cm}^2, \\ 8.5 \cdot 10^{20} (E/N)^{0.9} \text{ cm/s,} \\ \text{if } 4.01 \cdot 10^{-17} \text{ V} \cdot \text{cm}^2 < E/N \leq 7.61 \cdot 10^{-14} \text{ V} \cdot \text{cm}^2, \\ \frac{\exp\left(-\frac{10^{-10}}{3(E/N)^{0.81}}\right)}{\left(\frac{10^{-10}}{3} + 3.65 \cdot 10^{-17} (E/N)^{0.5}\right)} \text{ cm/s,} \\ \text{if } E/N > 7.61 \cdot 10^{-14} \text{ V} \cdot \text{cm}^2, \end{cases}$$

where N is the gas atom density;

$$u_{d,i}(E) = \mu_i(E) E_f \text{ cm/s;} \\ \mu_i(E) = 389 \exp\left(-\frac{E/N}{1.948 \cdot 10^{17}}\right) + 2136 \exp\left(-\frac{E/N}{2.105 \cdot 10^{18}}\right) + 1242 \exp\left(-\frac{(E/N)^{0.9}}{8.306 \cdot 10^{17}}\right)$$

$\text{cm}^2/(\text{V} \cdot \text{s})$ is the ion mobility; E_f is the strength near the channel front.

The ion diffusivity D_i was set as

$$D_i = \mu_i(E) T_g.$$

Here T_g (gas temperature) was taken equal to 0.03 eV; the electron diffusivity D_e was taken constant and equal to $1.5 \cdot 10^7 \text{ cm}^2/\text{s}$.

For the ionization rate v_i , the equation

$$v_i(E) = u_{d,e}(E) N \times \exp\left(-4.532 \cdot 10^{-16} \left(\frac{N}{E}\right)^{0.5} - 2.487 \cdot 10^{13} \frac{E}{N}\right) \text{ s}^{-1}$$

was used.

The boundary conditions for a system of equation on the internal and external electrodes were set as

$$\left. \frac{\partial N_i}{\partial r} \right|_{r=r_0} = 0, \quad j_e|_{r=r_0} = -\xi j_i|_{r=r_0}, \quad \phi|_{r=r_0} = -U_0; \\ j_e|_{r=r_{max}} = j_i|_{r=r_{max}} = 0, \quad \phi|_{r=r_{max}} = 0.$$

Here $\xi = 0.05$ determines the secondary electron yield.

The initial conditions for the field were chosen as follows:

$$E(r,t)|_{t=0} = E_0(r) = -U_0 \frac{r_0 r_{max}}{r_{max} - r_0} \frac{1}{r}; \\ \varphi(r,t)|_{t=0} = \varphi_0(r) = -U_0 \left[\left(\frac{1}{r_0} - \frac{1}{r} \right) / \left(\frac{1}{r_0} - \frac{1}{r_{max}} \right) \right].$$

Within the above diffusion-drift model, the plasma propagation speed, field distribution, and particle concentrations in the gap were calculated as functions of time. The curvature r_0 was chosen much less than r_1 (anode curvature): $r_0 \ll r_1$.

In the calculations, we took cathode curvature with $r_0 = 0.6 \text{ cm}$, anode curvature with $r_1 = 30 \text{ cm}$, and field strength $E \sim 10^5 \text{ V/cm}$. The background electron density in the inter-electrode space was set small; a bundle with an electron density of about 10^{16} cm^{-3} was modeled near the cathode, which approximately corresponded to the electron density N_e behind the BEMW front, following from the estimate $E = 2\pi e r_D N_e$ (here $r_D = (T_e/4\pi e^2 N_e)^{1/2}$ is the Debye radius; $T_e \sim 1 \text{ eV}$ is the electron temperature).

The time dependence of the wave front coordinate (Fig. 3) and front speed were calculated from the obtained distributions of electron and ion densities in different times (Fig. 2).

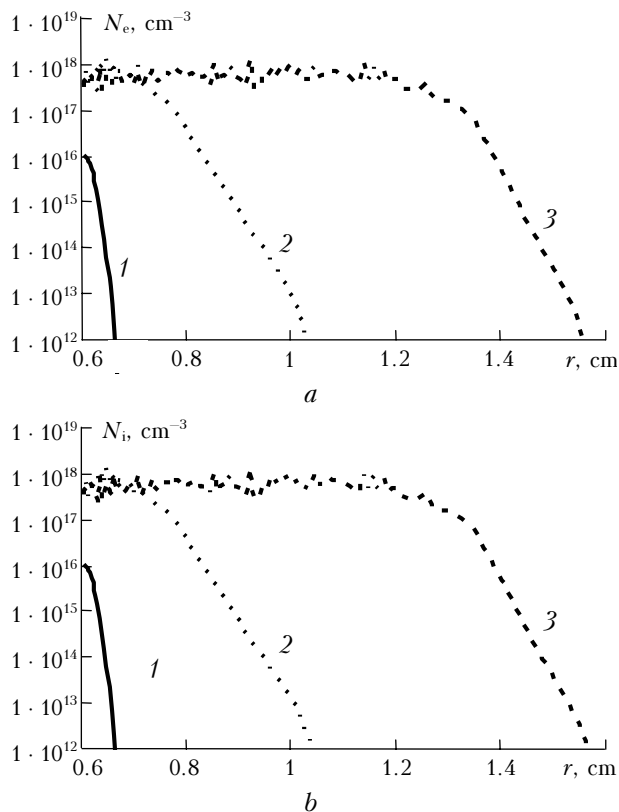


Fig. 2. Distribution of electron N_e (a) and ion N_i (b) density over the radius r for the negative BEMW at small cathode radius: $t_1 = 0$, $t_2 = 0.07$, $t_3 = 0.166$ ns, $p = 200$ torr, $N_{cr} = 10^{16}$ cm $^{-3}$, $E_0 \sim 10^5$ V/(cm · torr).

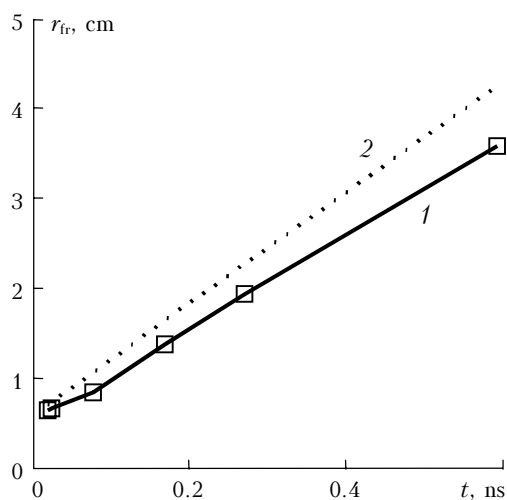


Fig. 3. Front radius r_{fr} as a function of t : calculations on the base of complete diffusion-drift model (1); approximation for the background multiplication model ($r_{fr} = u_{fr}t + \text{const}$, where $u_{fr} = 6.22 \cdot 10^9$ cm/s, $\text{const} = 0.6$ cm/s; $p = 200$ torr; $N_{cr} = 10^{16}$ cm $^{-3}$) (2).

In calculations on the base of the diffusion-drift model at parameters, given in Fig. 2, the average front

speed equals $5.1 \cdot 10^9$. This value is in good agreement with $6.2 \cdot 10^9$ cm/s, following from the analytical theory.

As is seen from Figs. 2 and 3, not only average speeds, but also the time dependences of wave front coordinates are in good agreement: the difference in coordinates, obtained by two models, does not exceed 20%.

Remind that the accuracy of the theory¹ is logarithmic (the logarithm of electron critical density enters into equations for characteristic parameters); hence, it is no sense to try for better agreement, e.g., improving the quality of approximations for values of the diffusion-drift model.

Conclusion

The use of the model of background electron multiplication in numerical simulation has shown that the BEMW speed in Ne is about 10^9 cm/s for the applied electric field $E/p \sim 10^5$ V/(cm · torr). The results of numerical simulation in the diffusion-drift approximation are in good agreement with BEMW speeds calculated by the analytical model; disagreement between the results does not exceed 20%.

References

1. S.I. Yakovlenko, in: *Communications on Physics* (GPI, 2003), No. 10, pp. 27–36.
2. S.I. Yakovlenko, *Pis'ma Zh. Tekh. Fiz.* **30**, No. 9, 12–20 (2004).
3. S.I. Yakovlenko, in: *Communications on Physics* (GPI, 2004), No. 2, pp. 22–28.
4. S.I. Yakovlenko, *Zh. Tekh. Fiz.* **74**, No. 9, 47–54 (2004).
5. S.I. Yakovlenko, in: *Short Message on Physics* (GPI, 2004), No. 12, pp. 35–41.
6. S.I. Yakovlenko, *Pis'ma Zh. Tekh. Fiz.* **31**, No. 14, 76–82 (2005).
7. G. Reiter, *Electron Avalanches and Gas Breakdown* (Mir, Moscow, 1968), 390 pp.
8. L. Leb, *Main Processes of Gas Discharging* (Gos. Izdat. Tekhniko-Teor. Lit., Moscow; Leningrad, 1950), 672 pp.
9. Yu.P. Raizer, *Physics of Gas Discharge* (Nauka, Moscow, 1992), 536 pp.
10. S.I. Yakovlenko, in: *Communications on Physics* (GPI, 2006), No. 2, pp. 10–16.
11. S.I. Yakovlenko, *Laser Phys.* **16**, No. 3, 403–426 (2006).
12. V.A. Gundienkov and S.I. Yakovlenko, in: *Communications on Physics* (GPI, 2006), No. 2, pp. 17–21.
13. V.A. Gundienkov and S.I. Yakovlenko, *Zh. Tekh. Fiz.* **76**, No. 9, 130–132 (2006).
14. V.F. Tarasenko and S.I. Yakovlenko, *Usp. Fiz. Nauk* **174**, No. 9, 49 (2004).
15. A.M. Boichenko and S.I. Yakovlenko, *Quant. Electron.* **36**, No. 12, 1176–1180 (2006).
16. A.N. Tkachev, A.A. Fedenev, and S.I. Yakovlenko, *Zh. Tekh. Fiz.* **75**, No. 4, 60–66 (2005).
17. A.N. Tkachev and S.I. Yakovlenko, *Laser Phys.* **13**, No. 9, 1–12 (2003).
18. Yu.I. Sytsko and S.I. Yakovlenko, *Laser Phys.* **6**, No. 5, 989 (1996).